Separation Science and Technology
Publication details, including instructions for authors and subscription information:
http://www.informaworld.com/smpp/title~content=t713708471

Sorption of Metals by an Amidoxime Chelating Resin. Part I: Equilibrium

Jose M. Loureiro; Alirio E. Rodrigues

To cite this Article Loureiro, Jose M. and Rodrigues, Alirio E.(1998) 'Sorption of Metals by an Amidoxime Chelating Resin. Part I: Equilibrium', Separation Science and Technology, 33: 11, 1585 — 1604
To link to this Article: DOI: 10.1080/01496399808545067
URL: http://dx.doi.org/10.1080/01496399808545067

SEPARATION SCIENCE AND TECHNOLOGY, 33(11), pp. 1585–1604, 1998

Sorption of Metals by an Amidoxime Chelating Resin. Part I: Equilibrium

LICÍNIO M. FERREIRA,* JOSÉ M. LOUREIRO,† and ALÍRIO E. RODRIGUES
LABORATORY OF SEPARATION AND REACTION ENGINEERING
SCHOOL OF ENGINEERING
UNIVERSITY OF PORTO
4099 PORTO CODEX, PORTUGAL

ABSTRACT

The complexation equilibrium of metals (copper, lead, and zinc) by using a chelating ion-exchange resin (Duolite ES-346) is analyzed. Two potentiometric titrations of the resin which allow evaluation of the exchange capacity and the pK values are carried out. Two equilibrium models (mass action type model and surface complex formation model) are proposed, and their parameters are estimated by fitting model equations to data from batch experiments. The degradation of the amidoxime groups in acidic media and a possible way to minimize that problem is discussed.

INTRODUCTION

Chelating resins represent an important category of synthetic copolymers of wide applicability to selectively remove toxic metal cations. In those resins the copolymer is usually styrene–divinylbenzene and the chelating agent is a functional group (iminodiacetic, sulfonic acid, amide, amidoxime, etc.) that forms strong complexes with such ions (1, 2). The high ion selectivities of chelating exchangers are attributed not only to electrostatic forces but also to coordination bonds in metal-chelating groups.

---

* Present address: Chemical Engineering Department, University of Coimbra, 3000 Coimbra, Portugal.
† To whom correspondence should be addressed.

For many wastewaters, the separation of one metal from another is often the first step to its recovery and reuse. Recovery of valuable metals such as gold, platinum, silver, copper, zinc, chromium, etc. by treating electroplating wastes, hydrometallurgical liquors, and mine wastewaters is becoming increasingly important on a commercial scale due to its economic and environmental benefits (3). Such a process is useful for metal waste control because it avoids environmental pollution. Recently, a new ion-exchange process for the selective removal, recovery and reuse of chromium from tannery wastes was developed by Petruzzelli et al. (4).

Extensive investigations have been carried out with chelating resins containing amidoxime groups. While alkali and alkaline earth metals are poorly retained by these resins, transition and other metal ions show quite different patterns of selectivity (5). Colella et al. (6) demonstrated that poly(acrylamidoxime) can be successfully used for the preconcentration of trace metals from aqueous solutions. The pH dependence of metal–resin chelation was determined for several metals in their work.

One of the best examples of the applicability of chelating resins for the concentration of tracer elements is the recovery of uranium from seawater (7–13). The concentration of uranium in seawater is about 3 mg/m^3 (14), and it exists mainly as the tricarbonatouranate (VI) ion, $[UO_2(CO_3)_3^{4-}]$ (15). In experimental studies carried out by Saito et al. (14), a concentration factor for uranium of more than 105 was found. Two further interesting examples of ion exchange with chelating resins are the recovery of gallium from Bayer liquors (16) and of mercury(II) from industrial wastewaters (17).

The present work reports on the sorption of copper, zinc, and lead from aqueous solutions with the commercial resin Duolite ES-346. Copper frequently exists in wastewaters generated in plants which treat mineral ores; the other metals are usually associated with copper minerals.

As in our previous works (18–20), the objective of this study was to better understand how pH influences the chelating ion-exchange process. It is known that in spite of the high affinity of the chelating resins toward metal ions, selective metal uptake is greatly impaired under highly acidic conditions (21).

Equilibrium data in batch systems and kinetic data in CSTR (to be reported in Part II) were obtained with the purpose of estimating the parameters to be used in the description of the behavior of fixed-bed ion-exchange columns.

This paper also analyzes some problems associated with the stability of the resin in acidic media, such as degradation of the amidoxime groups.

EXPERIMENTAL: MATERIALS AND PROCEDURE

Chelating Resin

The chelating resin used was Duolite ES-346, obtained from Dia-Prosim (France), a subsidiary of Diamond Shamrock Co. which now belongs to Rohm

TABLE 1
Physical Properties of Duolite ES-346 Resin

Matrix	Macrorecticular crosslinked
Wet density, kg wet resin/m^3 of dry resin	1100
Polymer density, kg polymer/m^3 of polymer	1150
Bulk density, kg dry resin/m^3 of bed	350
BET surface, m^2/g dry resin	49
Moisture content, wt%	50–60
Average pore diameter, nm	30

and Haas Co. This resin is a crosslinked copolymer (polystyrene–divinylbenzene) with amidoxime chelating groups having the formula

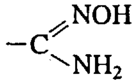

$$-C\begin{matrix}\nearrow NOH\\ \searrow NH_2\end{matrix}$$

It also contains a small proportion of hydroxamic acid (RCONHOH) groups which function in the higher pH range (22).

The resin was converted to the hydrogen form by elution with 0.1 N nitric acid and rinsed to neutral pH with distilled water. Its physical properties are shown in Table 1.

Potentiometric Titrations

Two potentiometric titrations were carried out. Experimental curves are presented in Figs. 1 and 2. With respect to the experiment shown in Fig. 1, fixed quantities of HNO_3 (0.12 N) were consecutively added to 0.311 g of dry resin in the Na-form (preconditioned by contact with a 1 N NaOH solution), immersed in 50 cm^3 of a NaCl neutral solution; enough time for equilibration was allowed between additions. Regarding the experiment shown in Fig. 2, 0.456 g of dry resin in the H-form immersed in 150 mL of distilled water were contacted with increasing quantities of NaOH (0.07 N). These experiments were performed at 25°C; the pH values shown in the figures are the equilibrium values after each addition.

Equilibrium Isotherms at 25°C

Equilibrium results presented in Figs. 3 and 4 were obtained by equilibrating over 15 days a given mass of resin Duolite ES-346 with 75 cm^3 of lead nitrate solution at 25°C containing 2 g/L of lead. After equilibrium was achieved, resin and solution were separated by filtration and all the ion species in solution were analyzed. The concentrations in the resin in equilibrium with

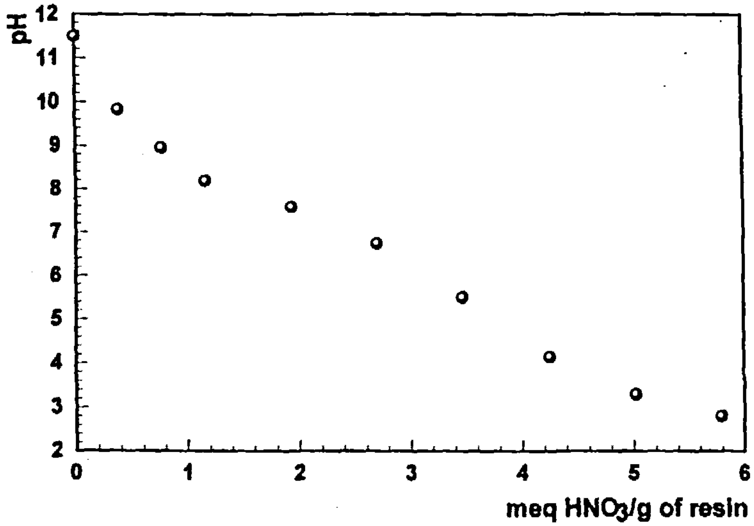

FIG. 1 Titration curve of Duolite ES-346 with 0.12 N nitric acid.

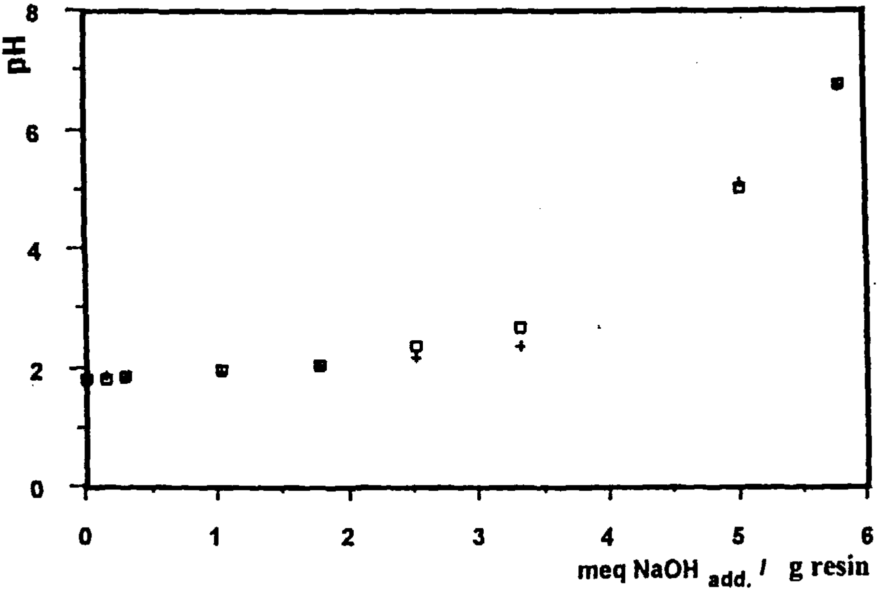

FIG. 2 Titration curve of Duolite ES-346 with 0.07 N sodium hydroxide: □, experimental; +, calculated with Eq. (16).

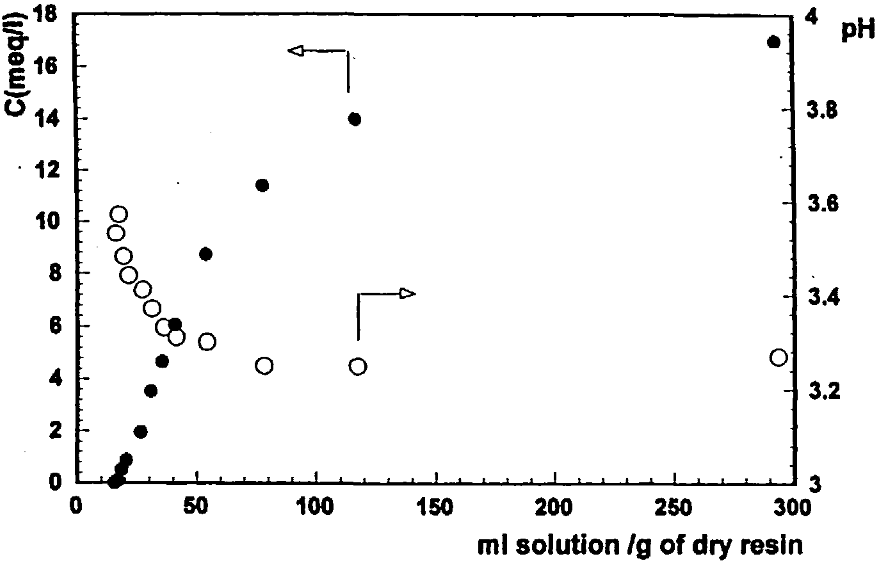

FIG. 3 Concentration of lead (●) and pH (○) in solution vs ratio volume of solution/mass of dry resin.

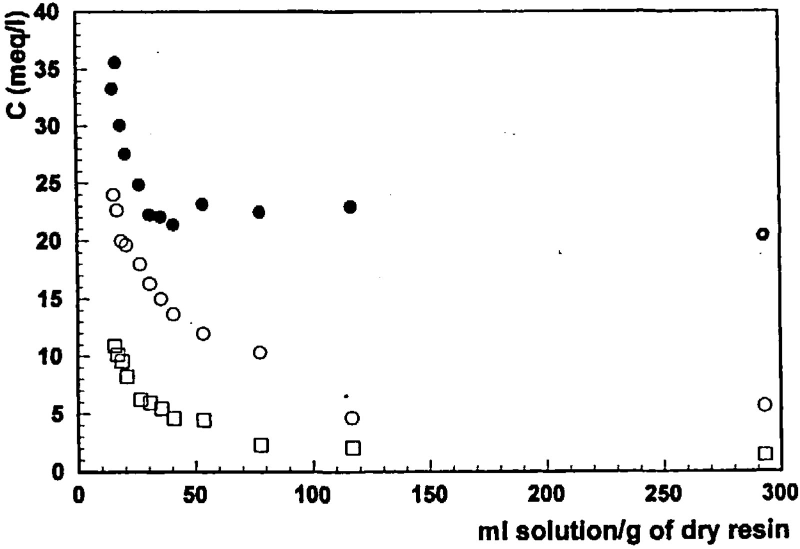

FIG. 4 Concentrations of nitrate (●), ammonium (□), and hydroxylammonium (○) in solution vs ratio volume of solution/mass of dry resin.

the measured solution concentrations were calculated by material balance; the figures show the isotherm equilibrium data for the metal cation and the pH (Fig. 3), the ammonium and hydroxylammonium ions and the co-ion nitrate (Fig. 4).

Chemical Analyses

Metal concentrations in the liquid phase were determined by atomic absorption spectrophotometry on a Model 902 Spectrophotometer from GBC Scientific Equipment (Dandenong, Victoria, Australia). An Ion Chromatograph Model 2000i/SP from Dionex (Sunnyvale, California, USA) was used for the determinations of ammonium and sodium; pH measurements were done with a Model 202 Crison (Barcelona, Spain) pH meter using a glass combined electrode, while nitrate concentrations were measured with a nitrate-selective electrode with a PVC matrix (23); hydroxylamine was determined by titration with potassium bromate (24).

RESULTS AND DISCUSSION

Quantitative Treatment of the Potentiometric Titration Curves

The analysis of the potentiometric titration data allowed calculation of the ion-exchange capacity. A value of 4.8 meq/g was found from the amount of NaOH added up to the point where the steep rise in pH occurs in the curve shown in Fig. 2. The same value was obtained from measurements of H^+ consumption after titration with nitric acid (see Fig. 1) was completed.

The titration curve corresponding to Fig. 1 seems to be representative of acid resins with two dissociation equilibria that, taking the amidoxime neutral species as RH, can be formulated as

$$RHH^+ \rightleftharpoons RH + H^+ \tag{1}$$

$$RH \rightleftharpoons R^- + H^+ \tag{2}$$

Figure 1 also shows that the first reaction occurs mainly at pH values under 7, the range of practical interest for the uptake of metal ions, where Reaction (2) is absent, i.e., the resin is all in the RH and RHH^+ forms. Then, for the titration with nitric acid in the region of $pH < 7$, mass balance equations can be written as

$$Q_r = [RH] + [RHH^+] \tag{3}$$

$$[RHH^+] + (V/M)([H^+]_1 + [OH^-]_0) = (V/M)([OH^-]_1 + [H^+]_0) \tag{4}$$

where the factor (V/M) represents the volume of solution (after titrant addition) per mass of dry resin. Subscripts 0 and 1 indicate initial (immediately after titrant addition) and final (equilibrium conditions) concentrations, respectively.

The concentrations [RH] and [RHH$^+$] in the resin can be calculated using Eqs. (3) and (4). With these values and the hydrogen ion concentration $[\overline{H^+}]$ inside the resin, the degree of dissociation $\alpha = [RH]/Q_r$ and the equilibrium constant $K_a = \alpha[\overline{H^+}]/(1 - \alpha)$ could be estimated. Unfortunately, $[\overline{H^+}]$ in the resin is not available; it can only be determined indirectly through the external pH using the Donnan relationship (25):

$$[\overline{H^+}][\overline{A^-}] = [H^+][A^-] \tag{5}$$

where A^- is the co-ion. Accordingly, for a given constant ionic strength (constant $[A^-]$), a new "external" equilibrium constant can be defined as $K = \alpha[H^+]/(1 - \alpha)$. It should be noted that this equilibrium constant varies with the ionic strength. The Henderson–Hasselbach plot, experimental pH vs $\log[\alpha/(1 - \alpha)]$, is shown in Fig. 5. In this figure the following relationship is also represented, with pK = 7.31 and n = 4.07, showing good agreement with the experimental values:

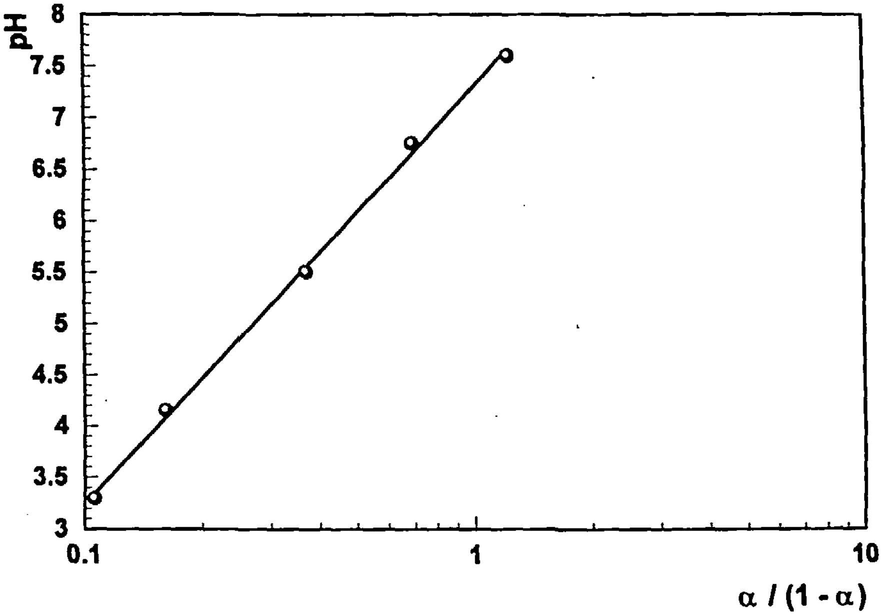

FIG. 5 Plot of pH against $\alpha/(1 - \alpha)$.

$$\mathrm{pH} = \mathrm{p}K + n \log\left(\frac{\alpha}{1 - \alpha}\right) \tag{6}$$

The value of the slope n deserves some comments. According to the definition of the "external" equilibrium constant, it should be equal to 1; its deviation from unity is generally attributed to electrostatic interactions of neighboring functional groups in the resin (25). Equation (6) can be used for computing the external pK. The second term in Eq. (6) vanishes when $\alpha = 0.5$ (50% conversion of the resin), so the external pK = 7.31 ($K = 4.86 \times 10^{-5}$ meq/L) for the experimental conditions of the titration shown in Fig. 1.

The next methodology leads to an estimate of the resin internal p$\overline{K}$ by treating the experimental data shown in Fig. 2. Assuming local equilibrium, ideality in the aqueous and solid phases and the absence of electrolyte adsorption, the titration behavior can be described with the aid of the following equations.

Resin dissociation:

$$\mathrm{RHH^+} \rightleftharpoons \mathrm{RH} + \overline{\mathrm{H}}^+ \tag{7}$$

Cation exchange:

$$\overline{\mathrm{H}}^+ + \mathrm{Na^+} \rightleftharpoons \overline{\mathrm{Na}}^+ + \mathrm{H^+} \tag{8}$$

Water dissociation:

$$\mathrm{H_2O} \rightleftharpoons \mathrm{H^+} + \mathrm{OH^-} \tag{9}$$

Equilibrium relationships:

$$K_{\mathrm{ai}} = \frac{[\mathrm{RH}][\overline{\mathrm{H}}^+]}{[\mathrm{RHH^+}]} \tag{10}$$

$$K_{\mathrm{i}} = \frac{[\mathrm{H^+}][\overline{\mathrm{Na}}^+]}{[\overline{\mathrm{H}}^+][\mathrm{Na^+}]} \tag{11}$$

$$K_{\mathrm{w}} = [\mathrm{H^+}][\mathrm{OH^-}] \tag{12}$$

Electroneutrality balances:

$$[\mathrm{Na^+}] + [\mathrm{H^+}] = [\mathrm{OH^-}] + [\mathrm{NO_3^-}] \tag{13}$$

Conservation of total fixed groups:

$$[\mathrm{RH}] = [\overline{\mathrm{H}}^+] + [\overline{\mathrm{Na}}^+] \tag{14}$$

$$Q_{\mathrm{r}} = [\mathrm{RH}] + [\mathrm{RHH^+}] \tag{15}$$

Quantities with overbars ($\overline{\mathrm{H}}^+$, $\overline{\mathrm{Na}}^+$) represent concentrations inside the resin.

According to Helfferich (1), neglecting specific interactions, swelling pressure effects, etc., $K_i \approx 1$ and then, given that the hydrogen ion concentration in solution is larger than the sodium concentration except at the very beginning of the titration, the same can be said about the concentrations inside the resin, i.e., the sodium concentration inside the resin can be taken as substantially higher than that of the hydrogen ion. Also, at pH < 7 the natural form of the resin is RHH^+; when the exchange Na^+/H^+ occurs, the released hydrogen ions are neutralized by the OH^- of the added hydroxide, maintaining a low H^+ concentration inside the resin; then, from Eq. (14), $[RH] \approx [\overline{Na^+}]$. Additionally, with Eqs. (10), (11), and (15) we get

$$[H^+] = \frac{K_{ai}(Q_r - [RH])[Na^+]}{[RH]^2} \qquad (16)$$

A $p\overline{K}$ value equal to 5.03 was obtained by the best fit of Eq. (16) to experimental data.

Estimation of Equilibrium Parameters

Numerical values of equilibrium parameters are needed for use in the description of the M^{2+}/H^+ binary exchange on Duolite ES-346 with the formation of a complex between the metal and the amidoxime group.

Two equilibrium reactions representing the resin dissociation and the complexing equilibrium of amidoxime can be written as follows:

$$RHH^+ \rightleftharpoons RH + H^+ \qquad (17)$$

$$2RH + M^{2+} \rightleftharpoons (RH)_2M^{2+} \qquad (18)$$

According to the mass action law, the equilibrium constants are given by

$$K_a = \frac{[RH][H^+]}{[RHH^+]} \qquad (19)$$

$$K_M = \frac{[(RH)_2M^{2+}]}{[RH]^2[M^{2+}]} \qquad (20)$$

On the other hand, the total concentration of ionized groups in the resin must be equal to the resin capacity Q_r; then,

$$Q_r = [RH] + [RHH^+] + [(RH)_2M^{2+}] \qquad (21)$$

Using Equations (19)–(21), the metal concentration in the resin $q_M = [(RH)_2M^{2+}]$ is given by

$$q_M = \frac{\left[2Q_r + \frac{\left(1 + \frac{C_H}{K_a}\right)^2}{K_M C_M}\right] - \sqrt{\left[2Q_r + \frac{\left(1 + \frac{C_H}{K_a}\right)^2}{K_M C_M}\right]^2 - 4Q_r^2}}{2} \tag{22}$$

where, for simplicity, $C_H = [H^+]$ and $C_M = [M^{2+}]$. Using the external $K_a = 4.86 \times 10^{-5}$ meq/L, previously calculated, K_M values were estimated by fitting Eq. (22) to experimental equilibrium data for copper, lead, and zinc on the Duolite ES-346 resin (18), using a Rosenbrock multivariable search, leading to $K_{Cu} = 2.03 \times 10^6$ g of resin $\times$ L of solution/meq^2, $K_{Pb} = 4.07 \times 10^4$ g of resin $\times$ L of solution/meq^2, and $K_{Zn} = 2.29 \times 10^2$ g of resin $\times$ L of solution/meq^2. A comparison between the experimental and calculated resin concentrations is shown in Fig. 6.

It should be noted that the experimental resin concentration was obtained by a material balance,

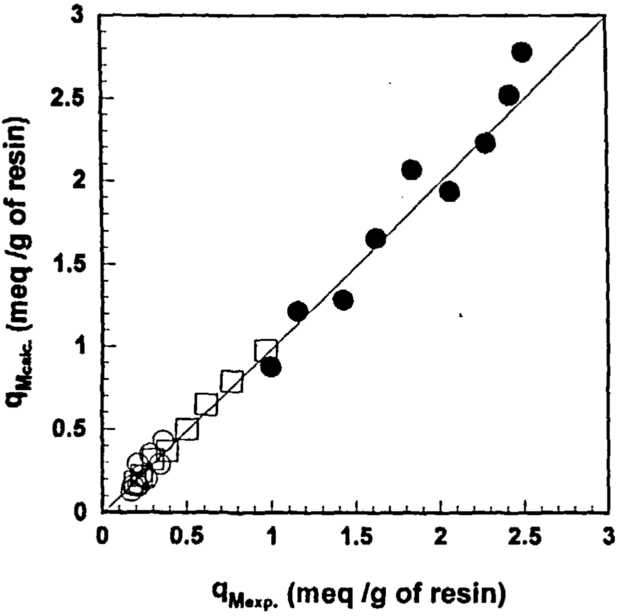

FIG. 6 Comparison between experimental, q_{Mexp}, and calculated, q_{Mcalc}, loading of resin at equilibrium: ●, Cu; □, Pb; ○, Zn.

$$q_M = [C_{Mo}V_f - C_M(V_f + V_h)]/m_s$$

where q_M (meq-g/g) and C_M (meq-g/L) are the metal concentrations in the resin and solution phases, respectively; C_{Mo} is the initial metal concentration in solution, V_f is the solution volume, V_h is the volume of water in the resin, and m_s is the dry resin mass.

Calculated values of the complexing equilibrium constants K_M show that copper is more strongly complexed than lead and zinc, as observed by Loureiro et al. (20). Nevertheless, the values of the equilibrium constants cannot be compared to the ones found previously since they have different units. This happens because, contrary to the previous treatment, now the dissociation equilibrium of the resin has been considered in order to quantify the uptake of protons competing with the metal toward the active sites in the resin. As the experiments were carried out at moderately acidic conditions (pH > 3), the complexation of the metal was favored corresponding to a K_a value compatible with an average degree of dissociation α.

An alternative strategy for the description of the chelation ion-exchange equilibrium, the surface complex formation model (26, 27), will be developed next. This model considers the ion exchanger resin matrix as a planar sheet with functional sites uniformly distributed over the surface. The electrical charge of the fixed sites is neutralized by counterions which are arranged in individual Stern layers. In a binary exchange system M^{2+}/H^+ there is only one Stern layer in which M^{2+} ions are located while protons are sorbed directly on the surface. Assume again the two equilibrium reactions:

$$RH + H^+ \rightleftharpoons RHH^+ \tag{23}$$

$$2RH + M^{2+} \rightleftharpoons (RH)_2M^{2+} \tag{24}$$

With the mass action law we get

$$K_H = \frac{[RHH^+]}{[RH][H^+]_s} \tag{25}$$

$$K_M = \frac{[(RH)_2M^{2+}]}{[RH]^2[M^{2+}]_s} \tag{26}$$

where the quantities $[H^+]_s$ and $[M^{2+}]_s$ are the concentrations in the surface plane and in a layer parallel to the surface, respectively. Concentrations in the free solution are obtained using the Boltzman relationship that gives the concentration as a function of the electric potential ϕ_x at a distance x from the surface (28).

For weak-acid exchangers, in which counterions in the diffuse layer can be neglected, the following relationship can be deduced (26, 27):

$$\log Q_{\mathrm{M,H}} = \log K_{\mathrm{M,H}} + 0.4343 \frac{2F^2 q_{\max}}{A_0 C_{\mathrm{ST}}(\mathrm{M,H})RT} y_{\mathrm{M}} \qquad (27)$$

where $Q_{\mathrm{M,H}} = q_{\mathrm{H}}^2 C_{\mathrm{M}}/(q_{\mathrm{M}} C_{\mathrm{H}}^2)$ is the selectivity coefficient, containing only quantities determined experimentally; in these equations, for simplicity, C_{M} and C_{H} are the metal and protons concentrations in the free solution; q_{M} and $q_{\mathrm{H}} = Q_{\mathrm{r}} - q_{\mathrm{M}}$ are the metal and protons concentrations in the resin. In Eq. (27) the second term contains only one variable, the fraction of the resin sites occupied by the metal, $y_{\mathrm{M}} = q_{\mathrm{M}}/Q_{\mathrm{r}}$; the other parameters are constants for a given isothermal ion-exchange: A_0 is the surface parameter, F is the Faraday constant, $C_{\mathrm{ST}}(\mathrm{M,H})$ is the electric capacitance of the Stern layer, R is the gas constant, and T is the absolute temperature.

Plotting $\log Q_{\mathrm{M,H}}$ vs y_{M} yields a straight line with slope

$$s = 0.4343 \frac{2F^2 q_{\max}}{A_0 C_{\mathrm{ST}}(\mathrm{M,H})RT}$$

and intercept equal to $\log K_{\mathrm{M,H}} = 2 \log K_{\mathrm{H}} - \log K_{\mathrm{M}}$.

Fitting Eq. (27) to experimental data for the binary exchange $\mathrm{Pb}^{2+}/\mathrm{H}^+$, such as is shown in Fig. 7, leads to $K_{\mathrm{M,H}} = 8.21$ and $s = 19.12$. The comparison

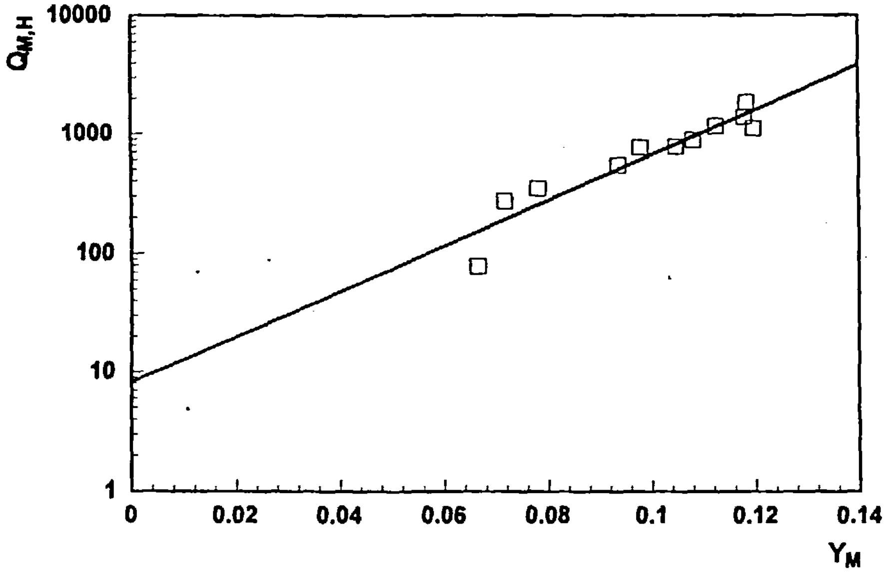

FIG. 7 Plot of $\log Q_{\mathrm{M,H}}$ against Y_{M} for the system Duolite ES-346/lead.

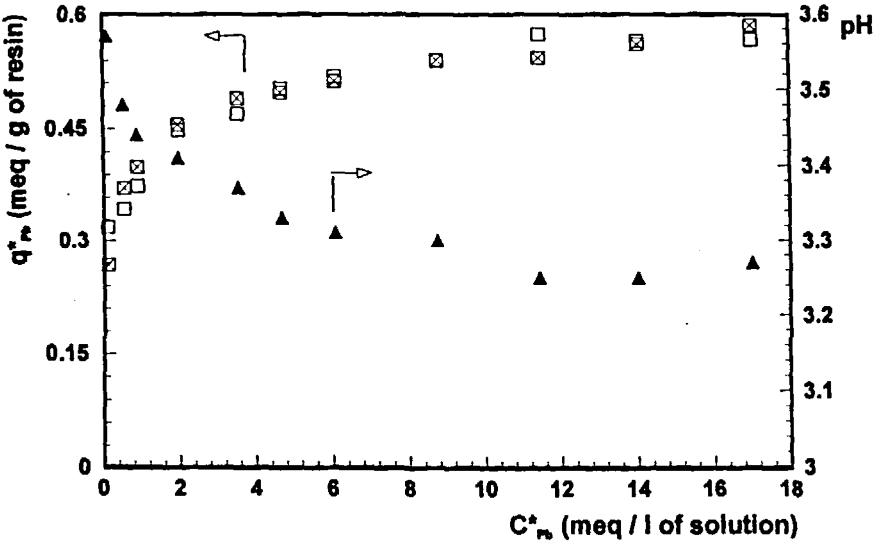

FIG. 8 Equilibrium isotherm at 25°C. System Duolite ES-346/lead: ☐, experimental; ☒, calculated with Eq. (27).

between experimental and calculated resin loading with lead is displayed in Fig. 8.

The same procedure was applied to the experimental data of Loureiro (18, 20) for the complexation of copper, lead, and zinc by the same resin (Duolite ES-346), and is shown in Fig. 9.

The following $K_{M,H}$ and s values were obtained:

Cu^{2+}/H^+: $K_{M,H} = 160.3$; $s = 0.34$

Pb^{2+}/H^+: $K_{M,H} = 9889$; $s = 0.24$

Zn^{2+}/H^+: $K_{M,H} = 1.3 \times 10^6$; $s = 3.01$

The larger differences between the calculated and the experimental values of log $Q_{M,H}$ occur in a region where the resin is weakly selective for the metal ($y_M < 0.1$). This is because the equilibrium is dominated in that region by counterions in the diffuse layer which were not taken into account in the derivation of Eq. (27) (26).

Comparing now the parameter values obtained, we can conclude that the resin complexes more strongly with the copper counterion since its $K_{M,H}$ value is the lowest, corresponding to a larger surface complex formation constant K_M. On the contrary, the zinc counterion is the less complexed with

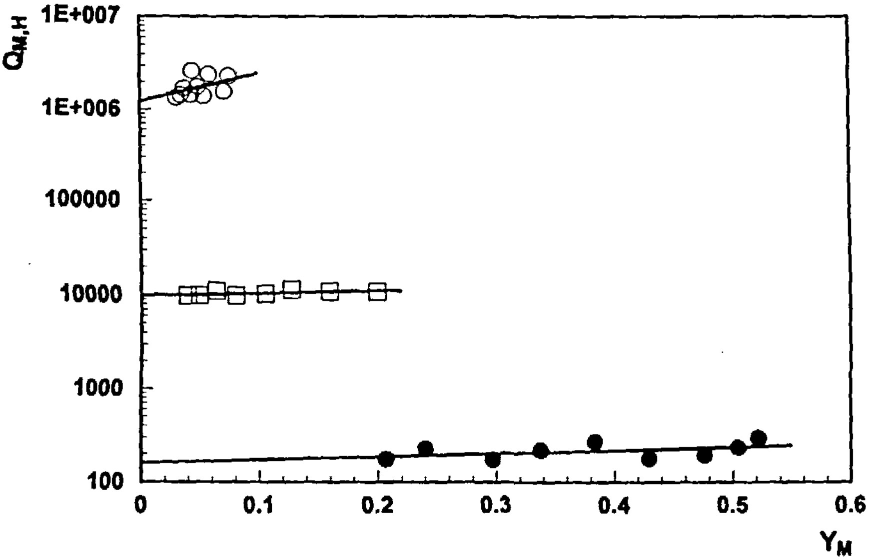

FIG. 9 Plot of log $Q_{M,H}$ against Y_M for the system Duolite ES-346/metal: ●, Cu; □, Pb; ○, Zn.

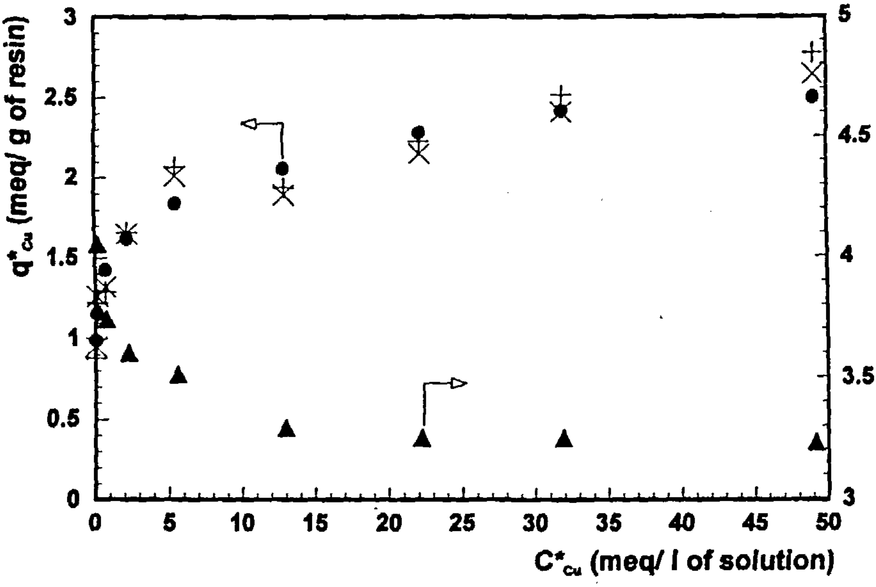

FIG. 10 Equilibrium isotherm at 25°C. System Duolite ES-346/copper: ●, experimental; +, calculated with Eq. (22); ×, calculated with Eq. (27); ▲, experimental pH.

greater slope *s*, indicating that the counterion is not as close to the surface. This is so because the slope is inversely proportional to the electric capacitance C_{ST}(M,H) which decreases with distance.

Regarding the complexation of lead, two straight lines of different slopes were found, one for each set of data. This probably happens due to the formation of two different types of surface complexes depending on the pH region where metal complexation occurs. Also, both sets of data fall in a region of low metal coverage ($y_M < 0.2$) where the counterions in the diffuse layer, neglected in the derivation of Eq. (27), dominate the equilibrium (26).

Figures 10 to 12 show the experimental loading of resin as a function of metal concentration in solution and those calculated with the two equilibrium models (mass action law and surface complex formation models) for the data of Loureiro (18, 20). It is seen that both models are able to represent the experimental results with reasonable accuracy, and that both models present larger relative deviations for zinc. These deviations between the experimental and calculated results for zinc can be attributed to the fact that the resin is less selective for this metal, as claimed before, resulting in a value of $y_M <$ 0.1 for all the experimental points, as shown in Fig. 9.

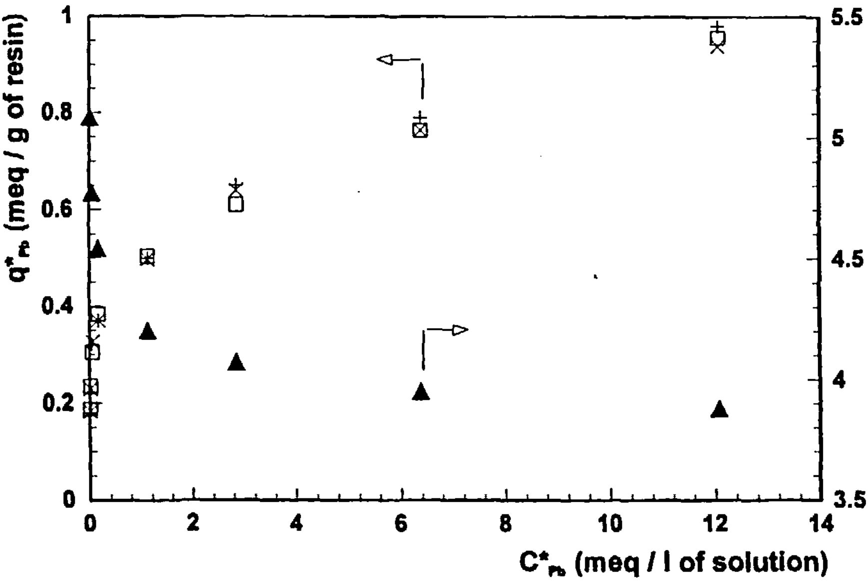

FIG. 11 Equilibrium isotherm at 25°C. System Duolite ES-346/lead: ☐, experimental; +, calculated with Eq. (22); ×, calculated with Eq. (27); ▲, experimental pH.

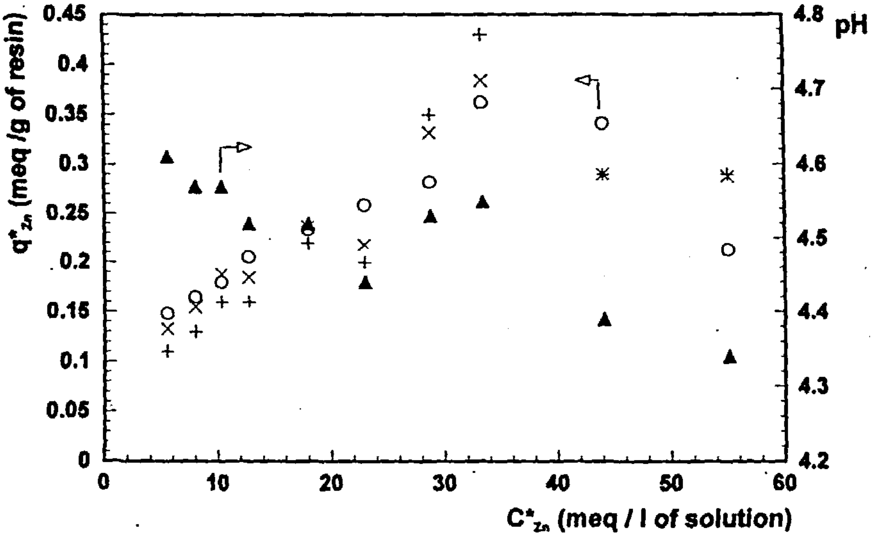

FIG. 12 Equilibrium isotherm at 25°C. System Duolite ES-346/Zn: ○, experimental; +, calculated with Eq. (22); ×, calculated with Eq. (27); ▲, experimental pH.

The Stability of Duolite ES-346

The presence of ammonium and hydroxylamine in solution in the experimental determination of equilibrium data for the complexation Pb^{2+}/H^+ on Duolite ES-346 (see Fig. 4) is an indicator of the degradation of amidoxime groups due to the instability of the resin in acidic media. This problem was reported by some authors (8, 9, 16, 29).

Two possible degradation reactions of amidoxime groups are represented by the following stoichiometric equations:

Reaction 1 (9):

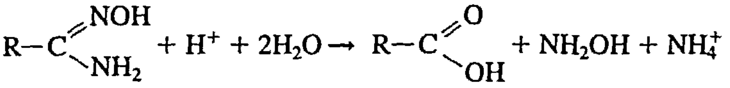

$$\mathrm{R{-}C}\begin{matrix}\mathrm{{/\!\!/}NOH}\\ \mathrm{\backslash NH_2}\end{matrix} + \mathrm{H^+} + \mathrm{2H_2O} \rightarrow \mathrm{R{-}C}\begin{matrix}\mathrm{{/\!\!/}O}\\ \mathrm{\backslash OH}\end{matrix} + \mathrm{NH_2OH} + \mathrm{NH_4^+} \qquad (28)$$

Reaction 2 (16):

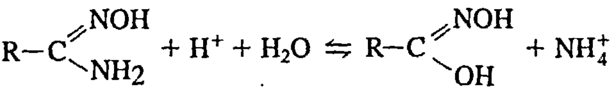

$$\mathrm{R{-}C}\begin{matrix}\mathrm{{/\!\!/}NOH}\\ \mathrm{\backslash NH_2}\end{matrix} + \mathrm{H^+} + \mathrm{H_2O} \rightleftharpoons \mathrm{R{-}C}\begin{matrix}\mathrm{{/\!\!/}NOH}\\ \mathrm{\backslash OH}\end{matrix} + \mathrm{NH_4^+} \qquad (29)$$

Reaction 2 is probably representative of the degradation of amidoxime groups in less acidic conditions than the necessary conditions for Reaction 1 to occur.

The transformation of amidoxime groups in acidic media is a serious problem which can significantly reduce the chelating capacity of the resin. Since the resin is more stable in neutral or slightly acidic solutions, contact with strongly acidic solutions should be avoided. Nevertheless, the regeneration of these resins is normally accomplished with such solutions, as suggested by the manufacturer (22). According to the very high conditional stability constants for the complexation of these metals with EDTA (30) in the range of pH values between 4 and 6, it seems that the possibility exists for the regeneration of the resin using a chelating reagent in weakly acidic conditions, instead of using strong mineral acids for metal recovery from Duolite ES-346.

CONCLUSIONS

The objective of this paper was the extension of previous studies (18–20) in order to describe the chelating equilibrium M^{2+}/H^+ on the Duolite ES-346 resin with more rigorous models. The resin dissociation equilibrium was introduced together with the metal complexation equilibrium, and this leads to a better understanding of the effect of pH on the chelating process.

At low pH values ($pH < 3.0$) the competition of H^+ ions for resin sites increases and the resin's chelating ability is greatly reduced. An increase in pH decreases the competition of H^+ ions for the resin sites, and complexation of the metal is favored. Two models were proposed, one based on the aforementioned competition and on the mass action law for the equilibrium description, and the other based on the surface complex formation theory (26, 27). It is shown that both models are able to describe the equilibrium with reasonable accuracy, enabling quantification of pH influence on the metal complexation equilibrium. They can then constitute a more rigorous basis for a mathematical description of the ion-exchange operation with chelating resins.

The instability of Duolite ES-346 in acidic media with degradation of the amidoxime active groups was observed. This degradation is more likely to occur during regeneration with strong mineral acids. The recovery of the complexed metals from the resin with a chelating reagent is suggested as an alternate regenerating strategy.

NOTATION

A_0	surface area parameter
C_{ST}	electric capacitance of Stern layers

F	Faraday constant
K	equilibrium constant
M	metal (Pb^{2+}, Cu^{2+}, or Zn^{2+})
q_i	concentration of ionized group i in resin phase
Q_r	resin capacity
R	gas constant
T	absolute temperature

Subscripts

a	acid
Cu	copper
M	metal
H	hydrogen
Pb	lead
r	resin
Zn	zinc

ACKNOWLEDGMENTS

Helpful comments from the reviewers are gratefully acknowledged; in the authors' opinion they definitely contributed to the improvement of the paper.

REFERENCES

1. F. Helfferich, *Ion Exchange*, McGraw-Hill, New York, NY, 1962.
2. A. Warshawsky, "Modern Research in Ion Exchange," in *Ion Exchange: Science and Technology* (A. E. Rodrigues, Ed.), Martinus Nijhoff Publishers, Dordrecht, 1986.
3. M. Streat, "Applications of Ion Exchange in Hydrometallurgy," in *Ion Exchange: Science and Technology*, (A. E. Rodrigues, Ed.), Martinus Nijhoff Publishers, Dordrecht, 1986.
4. D. Petruzzelli, R. Passino, and G. Tiravanti, "Ion Exchange Process for Chromium Removal and Recovery from Tannery Wastes," *Ind. Eng. Chem. Res.*, *34*, 2612–2617 (1995).
5. R. Dybczynski, Z. Hubicki, and K. Kulisa, "Ion Exchange Behavior of 23 Elements and Amphoteric Properties of Chelating Resin Duolite ES 346 Containing Amidoxime Groups," *Solv. Extr. Ion Exch.*, *6*(4), 699–724 (1988).
6. M. B. Colella, S. Siggia, and R. M. Barnes, "Synthesis and Characterization of a Poly(Acrylamidoxime) Metal Chelating Resin," *Anal. Chem.*, *52*(6), 967–972 (1980).
7. L. Astheimer, H. J. Schenk, E. G. Witte, and K. Schwochau, "Development of Sorbers for the Recovery of Uranium from Seawater. Part 2. The Accumulation of Uranium from Seawater by Resins Containing Amidoxime and Imidoxime Functional Groups," *Sep. Sci. Technol.*, *18*, 307–339 (1983).
8. F. Vernon and T. Shah, "The Extraction of Uranium from Seawater by Poly(Amidoxime)/Poly(Hydroxamic Acid) Resins and Fibre," *Reactive Polym.*, *1*, 301–308 (1983).

9. H. Omichi, A. Katakai, T. Sugo, and J. Okamoto, "A New Type of Amidoxime-Group-Containing Adsorbent for the Recovery of Uranium from Seawater. III. Recycle Use of Adsorbent," *Sep. Sci. Technol.*, *21*(6&7), 563–574 (1986).
10. K. Saito, T. Hori, S. Furusaki, T. Sugo, and J. Okamoto, "Adsorptive Characteristics of Uranium from Seawater Using Chelating Resins," in *3rd World Congress of Chemical Engineering, Tokyo*, 1986, pp. 683–686.
11. H. Omichi, A. Katakai, T. Sugo, and J. Okamoto, "Effect of Shape and Size of Amidoxime-Group-Containing Adsorbent on the Recovery of Uranium from Seawater," *Sep. Sci. Technol.*, *22*(4), 1313–1325 (1987).
12. T. Hirotsu, S. Katoh, K. Sugasaka, N. Takai, M. Seno, and T. Itagaki, "Adsorption of Uranium on Crosslinked Amidoxime Polymer from Seawater," *Ind. Eng. Chem. Res.*, *26*, 1970–1977 (1987).
13. M. Okazaki, "A Conceptual System Design for Uranium Recovery from Seawater Using Ocean Current and an Accelerated Method for Measuring Adsorption Equilibrium of Uranium," *Reports of Special Project Research on Energy*, Japan, 1987.
14. K. Saito, T. Hori, and S. Furusaki, "Porous Amidoxime-Group-Containing Membrane for the Recovery of Uranium from Seawater," *Ind. Eng. Chem. Res.*, *26*, 1977–1981 (1987).
15. T. Hirotsu, S. Katoh, K. Sugasaka, M. Seno, and T. Itagaki, "Adsorption Equilibrium of Uranium from Aqueous $[UO_2(CO_3)_3]^{-4}$ Solutions on a Polymer Bearing Amidoxime Groups," *J. Chem. Soc., Dalton Trans.*, pp. 1983–1986 (1986).
16. P. A. Riveros, "Recovery of Gallium from Bayer Liquors with an Amidoxime Resin," *Hydrometallurgy*, *25*, 1–18 (1990).
17. N. S. C. Becker and R. J. Eldrige, "Selective Recovery of Mercury(II) from Industrial Wastewaters. I. Use of a Chelating Ion Exchanger Regenerated with Brine," *Reactive Polym.*, *21*, 5–14 (1993).
18. J. M. Loureiro, "Adsorção e Reacção Química Simultâneas em Partículas Porosas: Aplicação ao Estudo da Recuperação de Metais com Resinas Complexantes," Ph.D. Thesis, Fac. Eng. Univ. Porto, 1986.
19. J. Loureiro, C. Costa, and A. Rodrigues, "Recovery of Copper, Zinc and Lead with Ion Exchange Complexing Resins in a CSTR Adsorber," in *Separation Technology* (N. Li and H. Strathmann, Eds.), Engineering Foundation, New York, NY, 1987, pp. 390–402.
20. J. Loureiro, C. Costa, and A. Rodrigues, "Recovery of Copper, Zinc and Lead from Liquid Streams by Chelating Ion-Exchange Resins," *Chem. Eng. Sci.*, *43*(5), 1115–1123 (1988).
21. Y. Zhu, E. Millan, and A. K. Sengupta, "Toward Separation of Toxic Metal(II) Cations by Chelating Polymers: Some Noteworthy Observations," *Reactive Polym.*, *13*, 241–253 (1990).
22. Diamond Shamrock Co., *Duolite CS-346 Technical Sheet*, Cleveland, OH, 1980.
23. J. L. F. C. Lima, A. A. S. C. Machado, A. Florido, S. Alegret, and J. M. Paulis, "Nitrate-Selective Electrode with PVC Membrane Applied to Electrically Conductive Epoxy," *Mem. Científica, Quím. Anal.*, *4*(2), 145–158 (1985).
24. A. I. Vogel, *A Textbook of Quantitative Inorganic Analysis Including Elementary Instrumental Analysis*, 3rd ed., Longmans, London, 1968.
25. R. L. Gustafson, H. F. Fillius, and R. Kunin, "Basicities of Weak Base Ion Exchange Resins," *Ind. Eng. Chem. Fundam.*, *9*, 221–229 (1970).
26. J. Horst, W. H. Holl, and S. H. Eberle, "Application of the Surface Complex Formation Model to Exchange Equilibria on Ion Exchange Resins—Part I. Weak Acid Resins," *Reactive Polym.*, *13*, 209–231 (1990).

27. W. H. Holl, J. Horst, and M. Wernet, "Application of the Surface Complex Formation Model to Exchange Equilibria on Ion Exchange Resins—Part II. Chelating Resins," *Ibid.*, *14*, 251–261 (1991).
28. A. W. Adamson, *Physical Chemistry of Surfaces*, Wiley-Interscience, New York, NY, 1990.
29. F. Vernon, "Chelating Ion Exchangers—The Synthesis and Uses of Poly(Hydroxamic Acid) Resins," *Pure Appl. Chem.*, *54*(11), 2151–2158 (1982).
30. A. Ringbom, *Complexation in Analytical Chemistry—A Guide for the Critical Selection of Analytical Methods Based in Complexation Reactions*, Wiley-Interscience, New York, NY, 1963.

Received by editor June 20, 1997
Revision received November 1997